CO_2 hydrogenation to olefins in microwave-thermal hybrid heating reactor

Sonit Balyan, Kshitij Tewari, Brandon Robinson, Changle Jiang, Yuxin Wang*, Jianli Hu*

Department of Chemical and Biomedical Engineering, West Virginia University, Morgantown, WV 26506, USA

*Corresponding Author: john.hu@mail.wvu.edu ; yuxin.wang1@mail.wvu.edu

Experimental Methods

The microwave assisted CO_2 hydrogenation to methanol were conducted in a Sairem microwave system, equipped with a 2.45 GHz solid state generator and 0.94 kw power. commercial catalyst $Cu/ZnO/Al_2O_3$ (HyKat SRK-50, CHEMPACK) was used in the reaction. A Micro-Epsilon pyrometer was positioned to measure the average temperature of the catalyst bed and control the microwave irradiation forward power. MeOH dehydration catalyst (SAPO-34, ACS Materials LLC, USA) was placed in the downstream of microwave system was heated using a furnace (Mellen, USA) equipped with a temperature control system. The feed gas mixture consisted of 60 vol.% He, 20 vol.% CO_2 balanced with N_2 for a total flow rate of 12 sccm is controlled using Brook mass flow controller. Prior to the hydrogenation reaction, $Cu/ZnO/Al_2O_3$ catalyst was reduced in gas mixture of 50 vol.% H_2 and 50 vol.% N_2 at 240 °C for 2 hours. The reduction temperature of the catalyst is measured by performing the temperature programmed reduction (TPR) experiment. A profile of the TPR is shown in Figure S1. A back pressure regulator was used to maintain the pressure in the reactor system. To hold the high pressure, a thick wall quartz tube reactor (8 mm-ID, 12 mm-ID) was used to carry out the reaction. The composition of the reactor outlet was analyzed by online gas chromatography (4-channel Inficon Fusion micro-GC). The reactor scheme of modular catalysis system is shown in Figure 1. It consists of two different reactor systems. The microwave reactor system was employed to carry out the CO_2 hydrogenation reaction for methanol production over the commercial $Cu/ZnO/Al_2O_3$ catalyst (1.5 gram). In the downstream of microwave reactor, the methanol conversion to olefins was carried out over the SAPO-34 catalyst (0.3 gram). The Results and Discussion section are divided into two sections. The first part covers the optimization of reaction parameters for

methanol production, while the second part focuses on the study of methanol conversion to olefins.

Reduction behavior of the calcined $Cu/ZnO/Al_2O_3$ if investigated by H-TPR. The sharp peak at 220 °C is attributed to the reduction of CuO[2]. The broader peak between 400-700C was ascribed to the ZnO reduction by the hydrogen spillover due to adjacent Cu[3].

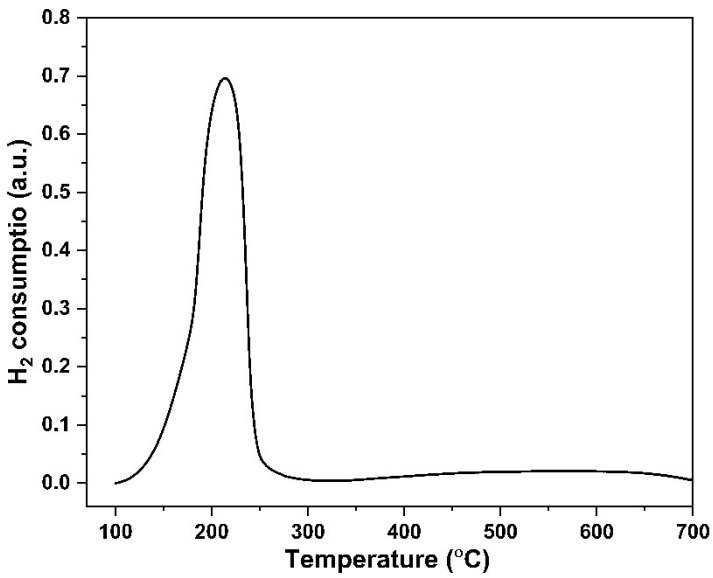

Figure S1. TPR profile of the calcined $Cu/ZnO/Al_2O_3$ catalyst

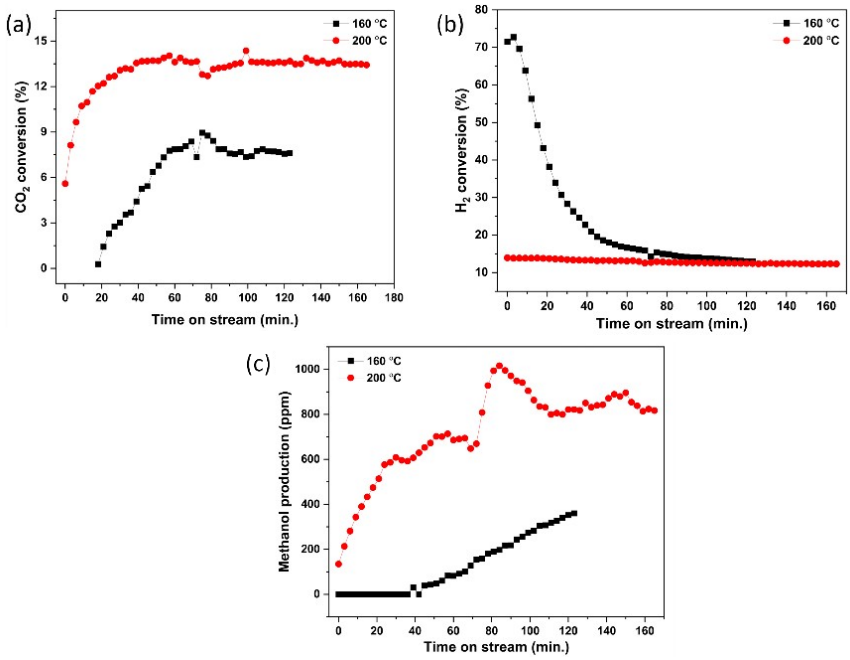

Figure S2. Effect of temperature on methanol production and H_2, CO_2 conversion [Process condition: Pressure: 80 psig, Catalyst weight: 1.5 gm, H_2:CO_2 ratio 3:1, Flow rate: 12.5 sccm

The data for conventional heating is recorded after 180 minutes of induction period. For conventional heating the CO_2 conversion is constant at ~ 20% after 40-minute TOS. Whereas the H_2 conversion decreases from ~35% at 60-minute TOS to 20% at 140-minute TOS. The production of methanol with conventional heating increases with TOS. At 60-minute TOS, the MeOH production is 2206 ppm, and it increases to 4200 ppm at 140-minute TOS. Under microwave heating the induction period is about 60 minutes. The CO_2 conversion varies between 13% and 14 %. H_2 conversion is constant at ~17% after 40-minute TOS. A maximum of 1015 ppm methanol production is observed at 90-minute TOS under microwave heating. Based on these studies for methanol synthesis, it is evident that the benefit of using microwave heating is that it reduces the induction period to 1/3 of the required time and the CO_2 can be converted to useful chemicals at moderate temperature and pressure.

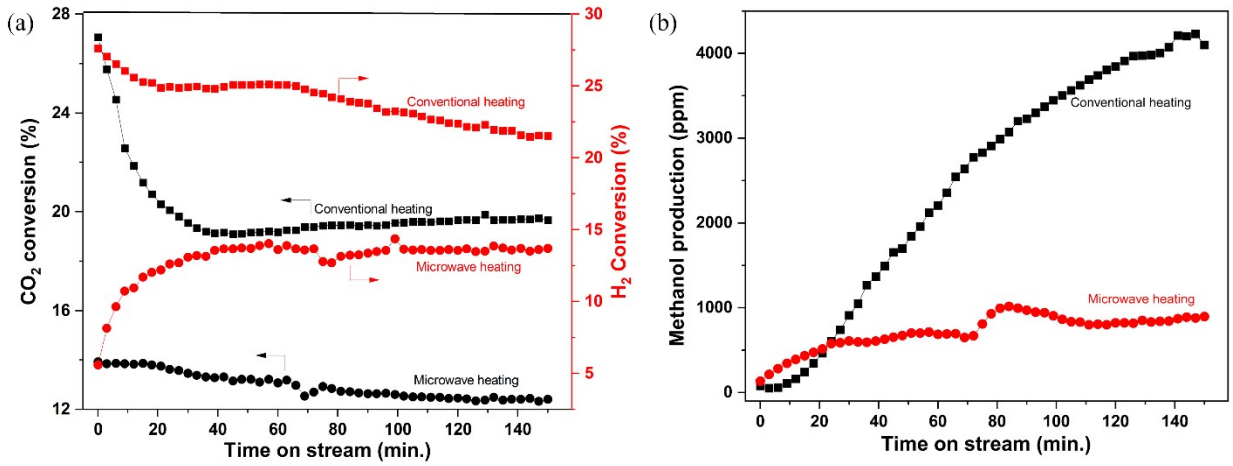

Figure S3. Catalytic performance of Cu/ZnO/Al_2O_3 catalyst for CO_2 hydrogenation (a) CO_2 and H_2 conversion, (b) methanol production (ppm). Process conditions: in conventional heating, pressure: 362 psig, temperature: 240 °C; in microwave heating, pressure: 80 psig, temperature: 200 °C. Catalyst weight: 1.5 gm, microwave power 0.4 kW, H_2: CO_2 ratio 3:1, flow rate: 12.5 sccm.

Figure S4 shows the effect of MTO reaction temperature on ethylene production. When the temperature is 400 C, no ethylene is observed in the reactor outlet. Only methanol presence in outlet stream is verified using online GC. When the temperature is increased to 425 °C only ethylene is observed in the product stream. Based on this 425 °C reaction temperature is chosen for MTO reaction.

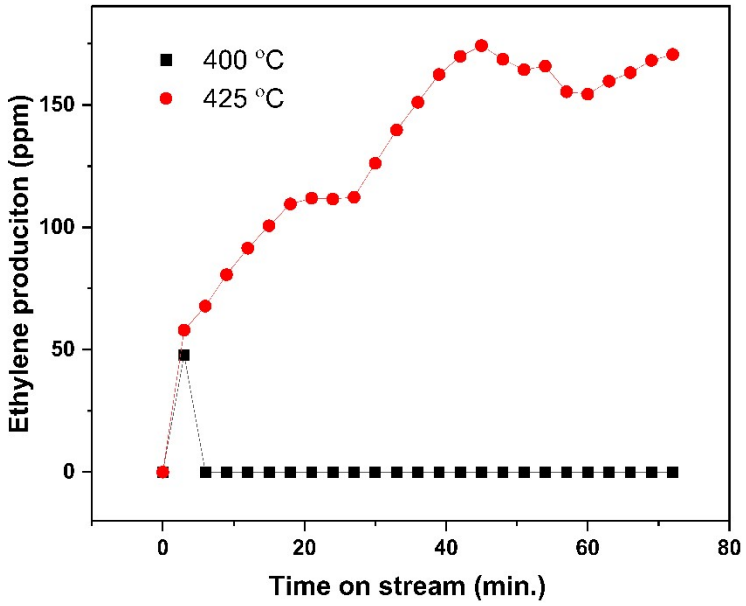

Figure S4. Effect of MTO reaction temperature on ethylene production

In calcined catalyst sample, clearly represented in inset (log scale), it is interesting that the diffraction peaks of CuO (identified as JCPDS# 00-041-0254) are prominently observed, whilst the diffraction peaks of ZnO (identified as JCPDS# 01-079-0205) are less intense but still recognizable. The peaks corresponding to CuO are detected at 2θ angles of 35.64°, 39.01°, 48.71°, 58.4° and 61.7°, whereas the peaks corresponding to ZnO are observed at 2θ angles of 32.4°, 56.58°, 66.09° and 68.168°. These peaks correspond to the crystal planes of CuO with Miller indices of (-1 1 0), (2 0 0), (-2 0 2), (2 0 2), and (-1 1 3) respectively and ZnO with Miller indices of (1 0 0), (1 1 0), (2 0 0), and (1 1 2) respectively. All the peaks of CuO and ZnO are slightly shifted to the right due to the amorphous nature of alumina. The absence of any discernible peak in the alumina sample suggests that it exists in an amorphous state. The dispersing effect of alumina leads to a rise in the relative intensity of diffraction peaks as the

value of alumina decreases. Furthermore, the evidence of a unique diffraction peak associated with graphite C (2θ = 26.4°, JCPDS#.01-089-8487) but very low intensity.

In other two catalyst samples at different temperatures 160° C and 200° C, the diffraction peaks associated with ZnO remain evident; however, the peaks related to CuO are no longer distinguishable. In contrast, the presence of distinct diffraction peaks at certain 2θ angles of 43.29°, 50.4°, 74.08°, 89.8°, and 95.04° can be observed, which are characteristic of metallic copper (PDF# 03-065-9743). These peaks correspond to the crystal planes of copper with Miller indices of (1 1 1), (2 0 0), (2 2 0), (3 1 1), and (2 2 2) respectively. The aforementioned process denotes the comprehensive conversion of CuO to Cu by means of exposure to a gaseous environment consisting of hydrogen (H2). Significantly, the condition of zinc oxide (ZnO) remains unchanged. Within the given context, it has been determined that Cu serves as the principal active site during the catalytic process involved in the synthesis of olefins from carbon dioxide. Furthermore, the evidence of a unique diffraction peak associated with graphite C (2θ = 26.4°, JCPDS#.01-089-8487) diminishes which clearly states that there is no graphitic carbon present in the catalyst. Significantly, the distinct diffraction peaks associated with Al2O3 are conspicuously absent in both reduced samples, indicating that Al2O3 may exist either in an amorphous state or in a highly scattered form within the catalyst matrix[7,8].

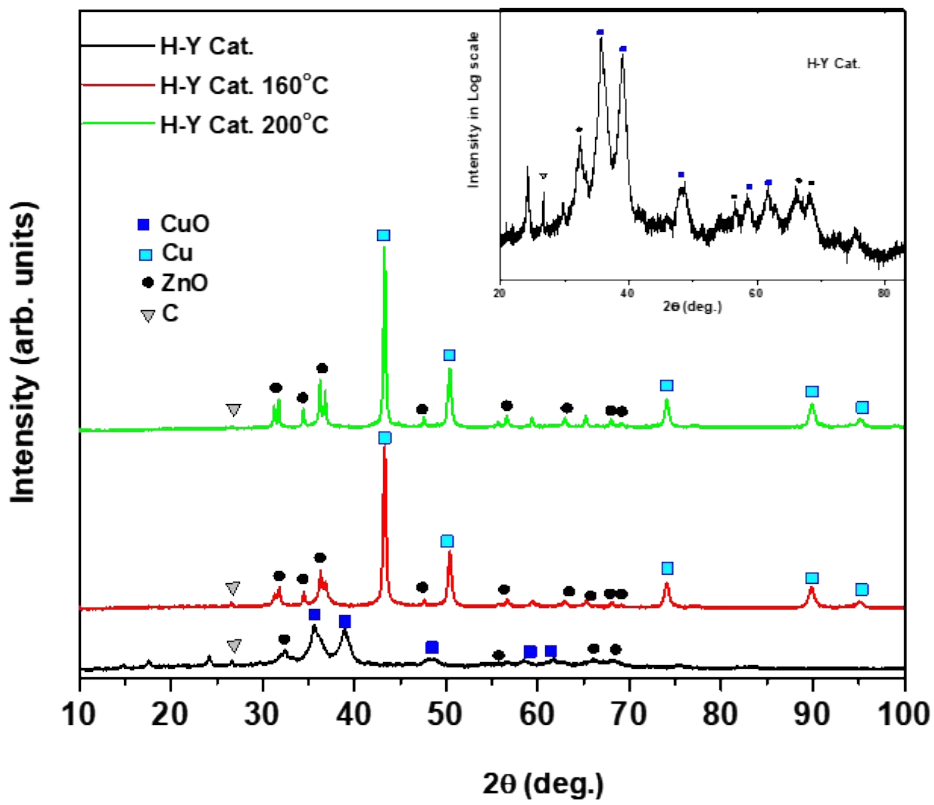

Figure S5. XRD of calcined and spent $Cu/ZnO/Al_2O_3$ catalyst.

Table S1. Effect of reaction temperature on Methanol production.

60-minute TOS				
	Conversion (%)		Production (ppm)	
Temperature(°C)	CO_2	H_2	MeOH	CO
160	7.8	16	82	1282
200	13.6	13	685	15491
120-minute TOS				
Temperature(°C)	CO_2	H_2	MeOH	CO
160	7.6	13.1	353	15845
200	13.6	12.5	821	19309

References

1 S. Balyan, C. Jiang, A. Caiola and J. Hu, *Chem. Eng. J.*, 2023, **454**, 140115.

2 F. Zhang, X. Xu, Z. Qiu, B. Feng, Y. Liu, A. Xing and M. Fan, *Green Energy Environ.*, 2022, **7**, 772–781.

3 B. Hu, Y. Yin, G. Liu, S. Chen, X. Hong and S. C. E. Tsang, *J. Catal.*, 2018, **359**, 17–26.

4 B. Xie, T. H. Tan, K. Kalantar-zadeh, J. Zheng, P. Kumar, J. Jiang, S. Zhou, J. Scott and R. Amal, *Appl. Catal. B Environ.*, 2022, **315**, 121599.

5 K. Lee, P. C. D. Mendes, H. Jeon, Y. Song, M. P. Dickieson, U. Anjum, L. Chen, T. C. Yang, C. M. Yang, M. Choi, S. M. Kozlov and N. Yan, *Nat. Commun.*, 2023, **14**, 1–11.

6 W. Karim, C. Spreafico, A. Kleibert, J. Gobrecht, J. Vandevondele, Y. Ekinci and J. A. Van Bokhoven, *Nature*, 2017, **541**, 68–71.

7 B. S. Clausen, G. Steffensen, B. Fabius, J. Villadsen, R. Feidenhans'l and H. Topsøe, *J. Catal.*, 1991, **132**, 524–535.

8 J. Yoshihara and C. T. Campbell, *J. Catal.*, 1996, **161**, 776–782.